#3820

Passive Solar Journal, 3(1), 33-76 (1986)

Natural Convection Research and Solar Building Applications

Ren Anderson
Solar Energy Research Institute
1617 Cole Boulevard
Golden, CO 80401

Abstract

The study of natural convection flows in enclosed spaces is one of the most active areas of heat transfer research today. Solar energy applications have provided a major stimulus for this research because of the importance of natural convection as a heat transfer mechanism in passive solar buildings and solar collectors. The results of this research are summarized and recommendations are made for future research areas that will result in further improvements in the performance of solar buildings.

INTRODUCTION

A passive solar system has been defined by Balcomb (1981) as "one in which the thermal energy flow is by natural means." Most passive designs use south-facing glass as the solar collection element and the building's structural mass as the thermal storage element. A successful passive design requires integration of the solar collection, thermal storage, and heat distribution functions into the architecture of the building. A thorough understanding of natural convection in enclosed spaces is absolutely necessary to successfully achieve this integration without sacrificing the comfort standard of conventional heat systems.

Passive applications range from small flat-plate thermosiphon collectors to various types of solar buildings components including Trombe walls, atria or sunspaces, and direct gain windows. Solar buildings can also incorporate vents or windows for ventilation cooling. As shown in the schematic diagrams of the main types of solar buildings in Figure 1, their geometries and thermal boundary conditions vary widely. In real applications, buildings are complicated further by the addition of furniture, draperies, and wall coverings.

This paper summarizes recent research findings on natural convection flows in enclosures from the viewpoint of solar building applications. This review focuses on the basic physical mechanisms that drive natural convection heat transfer in enclosures. Forced convection effects caused by air infiltration and natural ventilation through open doors and windows are not considered. Previous reviews of natural convection either have been general (Catton, 1978; Ostrach, 1982) or have been limited specifically to flat-plate solar collector applications (Buchberg, Catton, and Edwards, 1976). A recent review by Barakat (1985) summarizes research on natural convection between building zones, but does not examine the impact of natural convection on heat transfer through the building envelope or the effects of complicated building configurations.

In the following section, we describe some of the basic parameters that determine the characteristics of natural convection in solar buildings. We then review current research results relevant to natural convection effects on energy use at the building envelope,

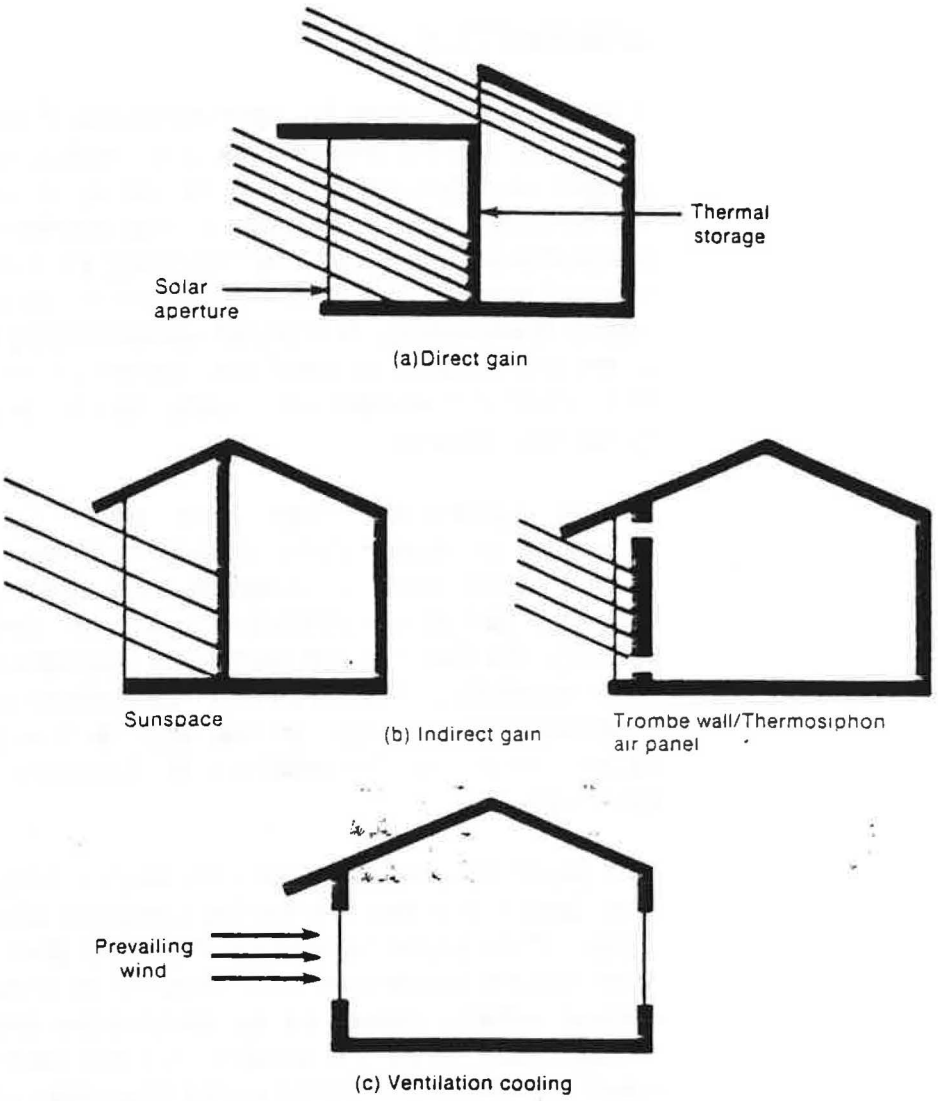

Figure 1. Schematic diagrams showing several types of solar buildings

natural convection within a single building zone, and convection between building zones.

We conclude the review by outlining important research areas in which our present understanding is incomplete.

CHARACTERISTICS OF NATURAL CONVECTION FLOW IN BUILDING GEOMETRIES

Window location and orientation are features of a passive solar home that distinguish it from a conventional home. A typical passive solar home has most of its windows on the south side. The thermal forcing produced by the absorption of solar energy and the presence of cold sinks, such as windows and thermal storage, produce strong free convection flows. These flows are the primary heat transfer mechanism between different building zones. Natural convection is also significant in determining the heat losses through external building surfaces and the heat transfer within single building zones.

Natural convection flows are created by density differences between the air at different locations inside a building. These differences are produced by differences between the temperatures of various building surfaces. Hot building surfaces result from solar illumination, auxiliary space heating systems, or thermal storage material that has been previously charged with heat. Cold surfaces result from windows, or thermal storage materials that have been discharged. South-facing windows and thermal storage materials can act as either cold sinks or hot sources, depending on the time. During the day, thermal storage materials act as cold sinks and south-facing windows act as hot sources. During the night, south-facing windows act as cold sinks and thermal storage materials act as hot sources. Natural convection flows are strongly influenced by building geometry and thermal boundary conditions. The overall objective of natural convection research has been to quantify the effects of surface temperature distributions and geometry on energy transport in natural convection applications.

To simplify the reporting of natural convection heat transfer results, they are commonly expressed in terms of nondimensional parameters. Nondimensional parameters provide a concise method of describing the geometry and surface temperature boundary conditions that influence the natural convection flow. The nondimensional parameters used in this review include:

the Rayleigh number

$$Ra = \frac{g\beta H^3 \Delta T}{\nu\alpha}, \qquad (1)$$

the flux modified Rayleigh number

$$Ra^{*} = \frac{g\beta H^{4} q}{\nu\alpha k} , \tag{2}$$

the Prandtl number

$$Pr = \frac{\nu}{\alpha} , \tag{3}$$

the room aspect ratio

$$A = H/L , \tag{4}$$

and the Nusselt number

$$Nu = \frac{\bar{h}H}{k} . \tag{5}$$

In Equations 1 through 5, g is the gravitational acceleration, β is the coefficient of thermal expansion, ΔT is the characteristic temperature difference, ν is the kinematic viscosity, α is the thermal diffusivity, k is the thermal conductivity, q is the surface heat flux, H is the height of the room, L is the length of the room, and $\bar{h}$ is the average natural convection heat transfer coefficient. The Nusselt number is a nondimensional heat transfer coefficient, the Rayleigh numbers define the temperature or heat flux boundary condition on a particular surface, the aspect ratio defines room geometry, and the Prandtl number defines the impact of fluid properties. Air has a Prandtl number of 0.7 and water has a Prandtl number of about 7. Prandtl number changes over the range $0.7 \leq Pr \leq 7$ affect average heat transfer results by only 10% to 15% when the flow is laminar (Bohn and Anderson, 1984).

The aspect ratio in building applications can be large or small. The Trombe wall is a large aspect ratio configuration with vertical parallel surfaces formed by the window and storage wall. Other types of solar buildings (sunspace, direct gain) have aspect ratios close to one. A number of thermal boundary conditions are possible, and many of them are quite complex. The Rayleigh numbers in building applications are on the order of 1×10^{10}. Depending on the specific application, the natural convection flow may be laminar, partially turbulent, or fully turbulent. For natural convection flows

next to a vertical heated or cooled surface at large Rayleigh numbers, velocity changes and air temperature changes are limited to a thin region directly adjacent to the surface (Figure 2). This near-wall region is known as a boundary layer. The air flows produced by all of the thermally active surfaces in a building combine to determine the overall natural convection circulation pattern in the building. Figure 3 shows schematic circulation patterns for two simple configurations. The boundary layers on heated and cooled surfaces combine to form a closed circulation loop that transports energy throughout the building.

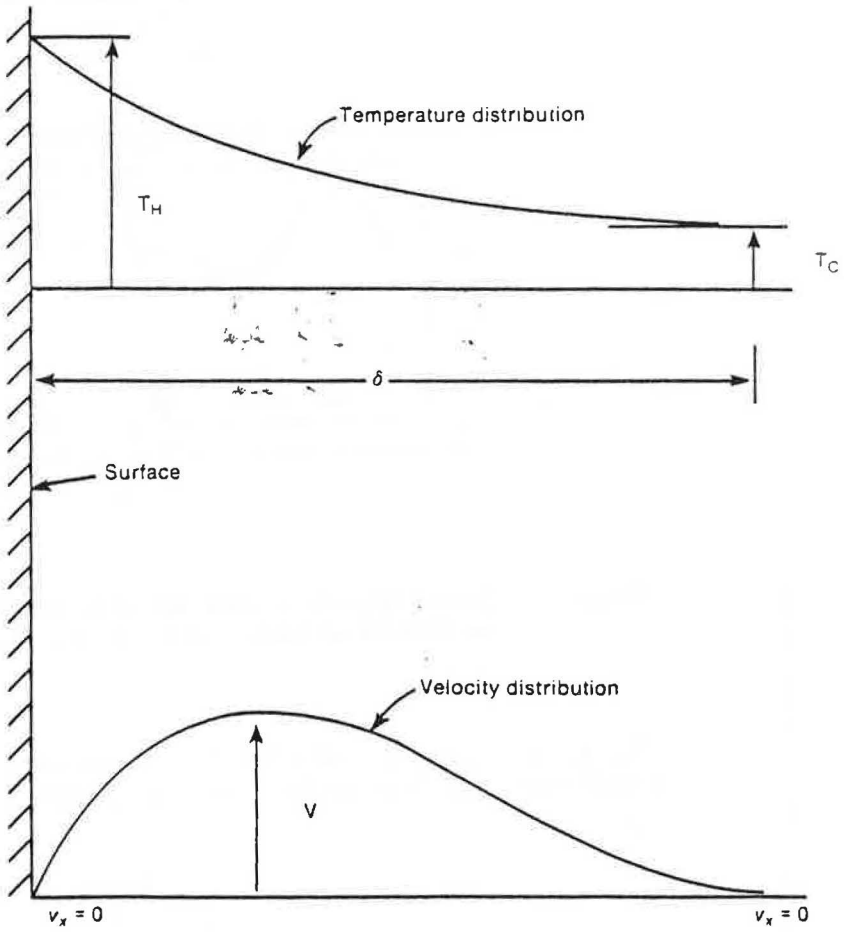

Figure 2. **Schematic diagrams showing temperature and velocity distributions in the natural convection boundary layer next to a heated vertical wall** Source: Chapman, 1974

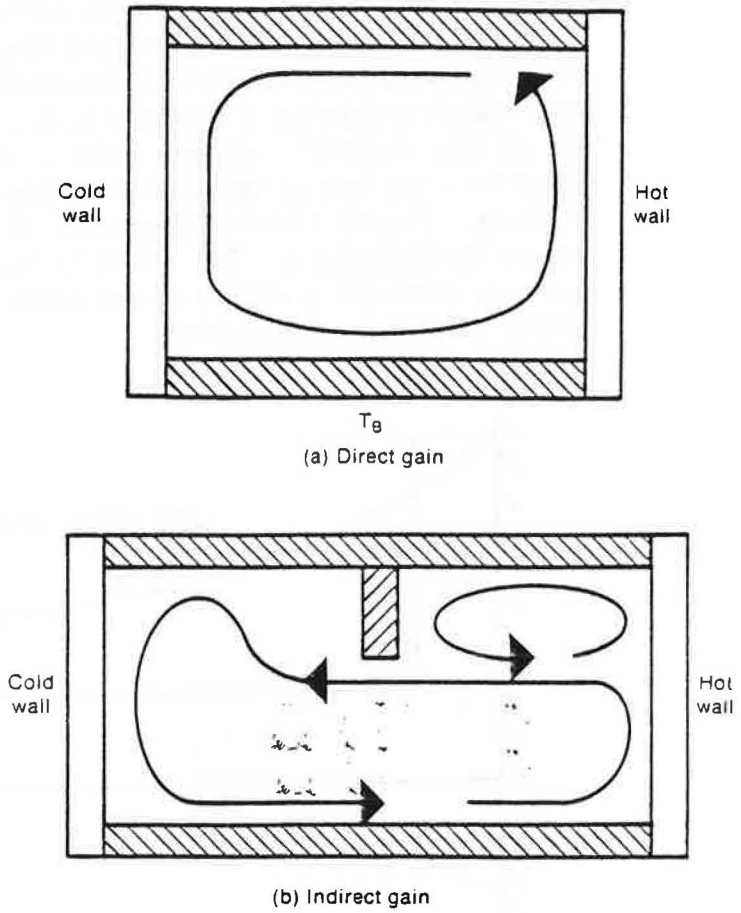

Figure 3. **Simple thermal models for solar building applications showing example circulation patterns** (see also Figure 1)

The air velocity, boundary layer thickness, and average heat transfer coefficient for laminar boundary layers can be estimated from the relations:

$$V \sim \frac{\alpha}{H} Ra^{1/2} , \tag{6}$$

$$\delta \sim \frac{H}{Ra^{1/4}} , \text{ and} \tag{7}$$

$$\bar{h} \sim \frac{k}{H} Ra^{1/4} \qquad (8)$$

where V and δ are the average air velocity and boundary layer thickness, respectively. In Equations 6 through 8, the temperature difference between the wall and room air is constant, and the room air is unstratified.

These simple relationships do not explicitly include the effect of room aspect ratio. Bejan (1980) has provided a synthesis of analytical results demonstrating the dependence of the Nusselt number on aspect ratio for laminar flow in two-dimensional enclosures with adiabatic horizontal walls. Figure 4 shows this dependence. The heat transfer is reduced in large aspect ratio enclosures because direct contact between the hot and cold surfaces is reduced as the aspect ratio increases. The heat transfer is also reduced in low aspect ratio enclosures but by a different physical mechanism. In low aspect ratio enclosures, the heat transfer is reduced as a result

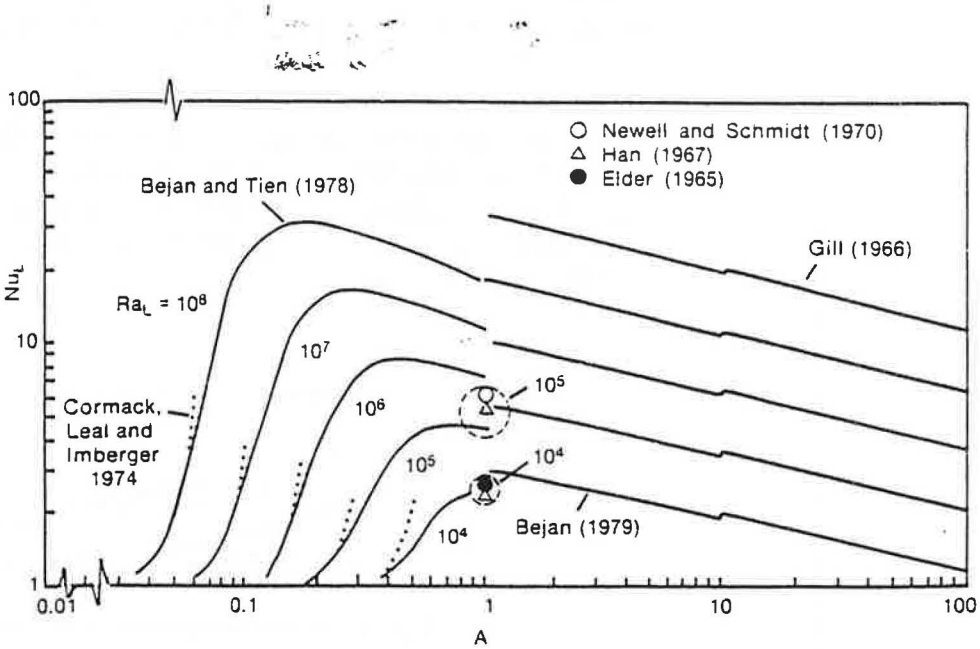

Figure 4. Effect of room aspect ratio A upon Nusselt number Nu in enclosures with heated and cooled end walls

of the increased drag produced by the presence of the horizontal boundaries. In enclosures with aspect ratios of one at high Rayleigh numbers, the primary effect of adiabatic horizontal boundaries is to turn the boundary layer flow created by the vertical walls. These turned boundary layers thicken and traverse the top and bottom of the enclosure.

NATURAL CONVECTION HEAT TRANSFER THROUGH THE BUILDING ENVELOPE

Single-Pane Windows

Numerous investigators have examined the combined natural convection/conduction heat transfer through a vertical surface that separates reservoirs at different temperatures. Studies by Lock and Ko (1973), Anderson and Bejan (1980), and Viskanta and Lankford (1981) examined heat transfer through a vertical plate separating semi-infinite fluid reservoirs. Sparrow and Prakash (1981) conducted a numerical investigation of an enclosure that was coupled via a conductive wall to an external natural convection flow.

Figure 5 compares the relative importance of indoor radiation and convection heat losses through a single-pane window as a function of indoor-outdoor temperature difference and external wind velocity. Figure 6 shows schematic flow patterns for each case. In each case the radiation component is roughly the same size as the natural convection component.

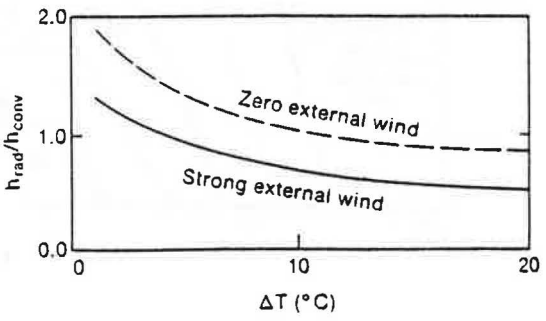

Figure 5. Relative importance of radiation and convection losses through a single-pane window as a function of indoor-outdoor temperature difference and wind velocity

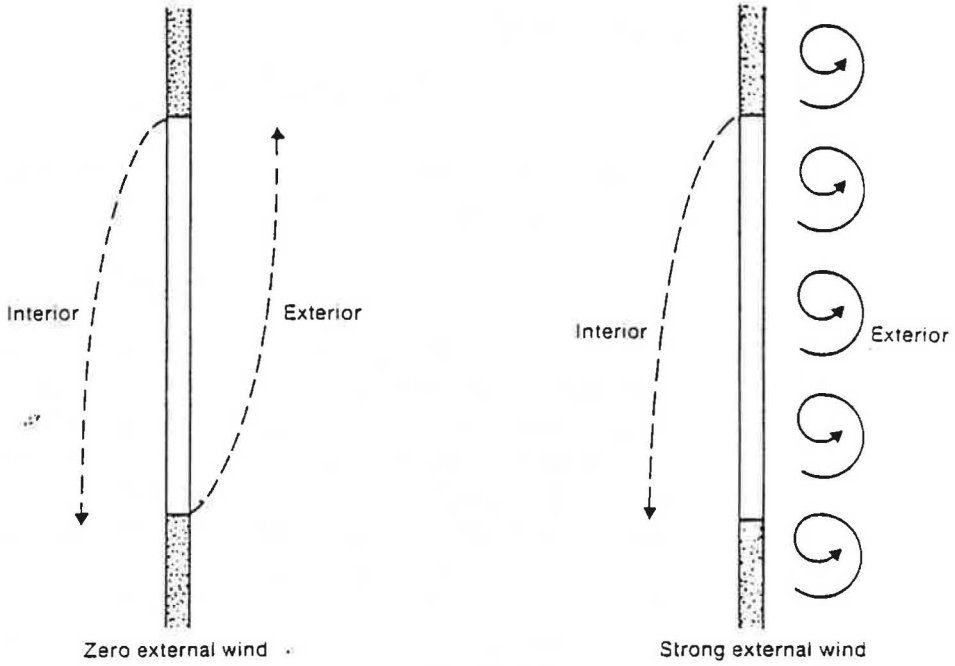

Figure 6. Air flow patterns for convection heat transfer through a single-pane window (arrows indicate direction of flow)

Double-Pane Windows

Almost all new construction in the United States uses double-pane windows because of their superior insulating qualities. Korpela, Lee, and Drummond (1982) have carried out a series of numerical experiments on large aspect ratio enclosures for the specific application of double-pane windows. They were primarily interested in determining the optimum spacing between the panes for minimum heat loss. As the spacing between the windows was reduced at constant window height, the flow in the cavity exhibited in succession a conduction-dominated unicellular flow, a multicellular flow, and finally reverted to a unicellular flow. The final unicellular flow was not a boundary layer flow but was in the transitional regime between conduction- and convection-dominated heat transfer. The minimum heat transfer was found to occur at the onset of the final multicellular flow. Korpela, Lee, and Drummond suggest the following formula for calculating the optimum aspect ratio for minimum natural

convection and conduction heat transfer as a function of the Rayleigh number:

$$A^3 + 5A^2 = 1.25 \times 10^{-4}\ Ra/Pr\ . \qquad (9)$$

For the high-aspect ratios typical of window applications, Equation 9 can be simplified to the form

$$L_{opt} = 20\ \left(\frac{\nu\alpha}{g\beta\Delta T}\right)^{1/3}\ . \qquad (10)$$

Equation 10 indicates that the optimum window spacing for minimum convective and conductive heat transfer is independent of the window height and inversely proportional to the temperature difference raised to the one-third power. For an air temperature difference of 10°C (18°F) this optimum spacing can be calculated to be ≈2 cm (0.8 in.). ElSherbiny, Raithby, and Hollands (1982) have conducted an extensive series of experiments in large aspect ratio enclosures that are consistent with the height independence predicted by Equation 10. They found that for A > 40 the transition between conduction- and convection-dominated heat transfer was independent of the aspect ratio, when the enclosure spacing was held constant.[2]

NATURAL CONVECTION WITHIN A SINGLE BUILDING ZONE

Heating and Cooling of Vertical Surfaces

The thermal boundary conditions in passive solar applications are generally three-dimensional, include heating and cooling of several walls at one time, and involve heating conditions that span the range from constant temperature surfaces to constant heat flux surfaces.

Balvanz and Kuehn (1980) have shown that the effect of finite wall conductivity can be significant, particularly for the case of a constant flux boundary condition. On a heated vertical wall subjected to a constant flux boundary condition, the temperature of the wall must increase with vertical location to maintain a constant driving temperature difference between the wall and the fluid in the boundary layer next to the wall. Conduction in the wall reduces the wall temperature gradient and produces a corresponding decrease in heat transfer from the wall. Figure 7 shows the wall temperature profile

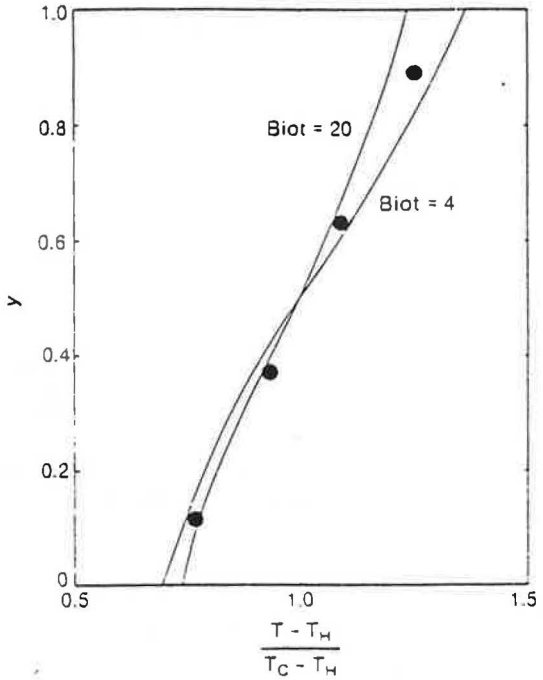

Figure 7. Effect of wall Biot number upon wall temperature distribution for a constant flux boundary condition

in a wall with Bi = 10 as measured by Anderson and Bohn (1984). Figure 8 shows the corresponding decrease in heat transfer predicted by Balvanz and Kuehn. The quantity Bi is the Biot number, a non-dimensional expression for the thermal conductivity of the wall. Large Biot numbers imply large wall thermal conductivity.

MacGregor and Emery (1969) conducted numerical calculations of natural convection flow in an enclosure and varied the thermal boundary condition on the heated wall. They found that convective heat transfer for a constant flux condition was 30% higher than when the heated wall was isothermal. The average temperature difference between the hot and cold wall was used in the definition of the Nusselt number for the constant flux surface. Schinkel and Hoogendoorn (1983) repeated the calculations of MacGregor and Emery for $Ra_L = 5.8 \times 10^4$ and found an increase of 20%. This prediction was found to agree with experiments done in air. Schinkel and Hoogendoorn have also done experimental comparisons

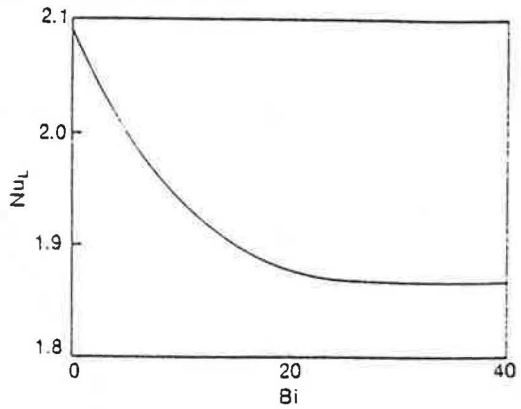

Figure 8. Effect of wall Biot number upon wall heat transfer for a constant flux boundary condition

at θ = 60°, 40°, and 20° and found increases of 15%, 11%, and 9%, respectively, where θ is tilt angle of the enclosure with respect to the horizontal.

Depending on window spacing, direct solar gain may result in a series of localized heated areas rather than uniform heating of an entire wall. Jaluria (1982) conducted a numerical study of the interaction of multiple horizontal heated strips on a vertical surface in the boundary layer regime. He found that the velocity increased and the temperature decreased as one moved downstream from the region of heating. Heat transfer from upstream heaters was enhanced if they were far enough upstream to benefit from the velocity produced by downstream heaters without being exposed to hot fluid. Kubleck, Marker, and Straub (1980) examined convection in enclosures with nonuniformly heated walls. They conducted a two-dimensional transient numerical analysis of a square box with one vertical wall heated on its lower half and cooled on its upper half. All other walls were insulated. The unstable stratification produced by this heating and cooling arrangement resulted in two vertically displaced convection cells that grew and decayed with time. Chao, Ozoe, and Churchill (1981) investigated theoretically the effect of sawtooth variations in the temperature of an inclined enclosure with an aspect ratio (H/L) of two. They found that the surface temperature variations produced a stronger circulation and a higher overall Nusselt number than did a uniform temperature.

Natural convection flows in enclosures differ from external natural convection flows because the flow recirculates and thus interacts with itself. It is difficult to model this interaction accurately through the use of external flow results applied to internal flows with the same surface temperature. However, it has been common practice to calculate building heat loads based on external flow results because detailed enclosure flow results did not exist until recently. Bauman, Gadgil, Kammerud, Altmayer, and Nansteel (1983) compared the correlations resulting from these two approaches and found the loads calculated from enclosure results to be 30% to 50% lower than results based upon correlations for isolated surfaces. Altmayer, Gadgil, Bauman, and Kammerud (1983) conducted a series of numerical experiments aimed at developing an improved set of correlations. They succeeded in providing a series of correlations that improved the other existing methods; however, the correlations are also substantially more complicated than existing methods.

Bohn, Kirkpatrick, and Olsen (1984) examined heat transfer in a cubical enclosure with heating and cooling of multiple vertical walls. They found that the heat transfer within the enclosure for any combination of hot and cold walls could be based on the area-weighted bulk temperature difference,

$$\Delta T_b = |T_i - T_b| \tag{11}$$

where

$$T_b = \frac{\Sigma_i T_i A_i}{\Sigma_i A_i} \tag{12}$$

and T_i and A_i are the temperature and the area, respectively, of surface i.

By using ΔT_b to define the heat transfer coefficient, Bohn, Kirkpatrick, and Olsen could express the heat transfer results for all of their experiments by one correlation. Bohn and Anderson (1986) subsequently found that the bulk temperature defined by Equation 12 closely predicted the measured average core temperature in a cubical enclosure with three-dimensional thermal boundary conditions on its vertical walls. This result is important because it demonstrates that the heat transfer in the boundary layer regime in an

enclosure with complicated thermal boundary conditions on the vertical walls is driven by the temperature difference between a given surface and the bulk fluid temperature in the core of the enclosure.[3]

Heating and Cooling of Horizontal and Vertical Surfaces

In building applications the floor and ceiling, like the walls, can be active heat transfer surfaces. The temperature distributions on the floor and ceiling can profoundly affect the flow patterns, thermal stratification, and heat transfer.

Ostrach and Raghavan (1979), Fu and Ostrach (1981), Shiralkar and Tien (1982), and Kirkpatrick and Bohn (1983 and 1986) have examined the effect of vertical- as well as horizontal-wall-temperature differences on natural convection in enclosures with four active heat transfer surfaces. Figure 9 shows cross-sections of the thermal boundary conditions that were used in these studies.[4]

Ozoe, Mouri, Hiramitsu, Churchill, and Lior (1984); Anderson, Fisher, and Bohn (1985a); and Anderson and Lauriat (1986) have examined the effects of heating and cooling of horizontal and vertical surfaces in enclosures for the case when less than four surfaces are thermally active. Ozoe et al. studied natural convection in a single building zone with a heated floor and a vertical wall that was cooled over 57% of its length. They conducted numerical calculations using a two-equation model of turbulence for $Ra = 10^6$ and found the flow to be weakly three dimensional with a horizontal boundary layer next to the heated floor. Ozoe et al. did not consider the heat transfer aspects of the problem.

Anderson and Lauriat conducted a numerical study of natural convection in a closed cavity with an isothermal vertical wall that was cooled over its entire length, and a heated floor. The heat transfer and flow patterns were calculated for cases when the floor was isothermal as well as for cases when the floor was a constant heat flux surface. A horizontal boundary layer was found to form next to the heated floor, in agreement with numerical calculations by Ozoe et al. and experimental observations by Anderson, Fisher, and Bohn (1985a). The structure of the horizontal boundary layer calculated

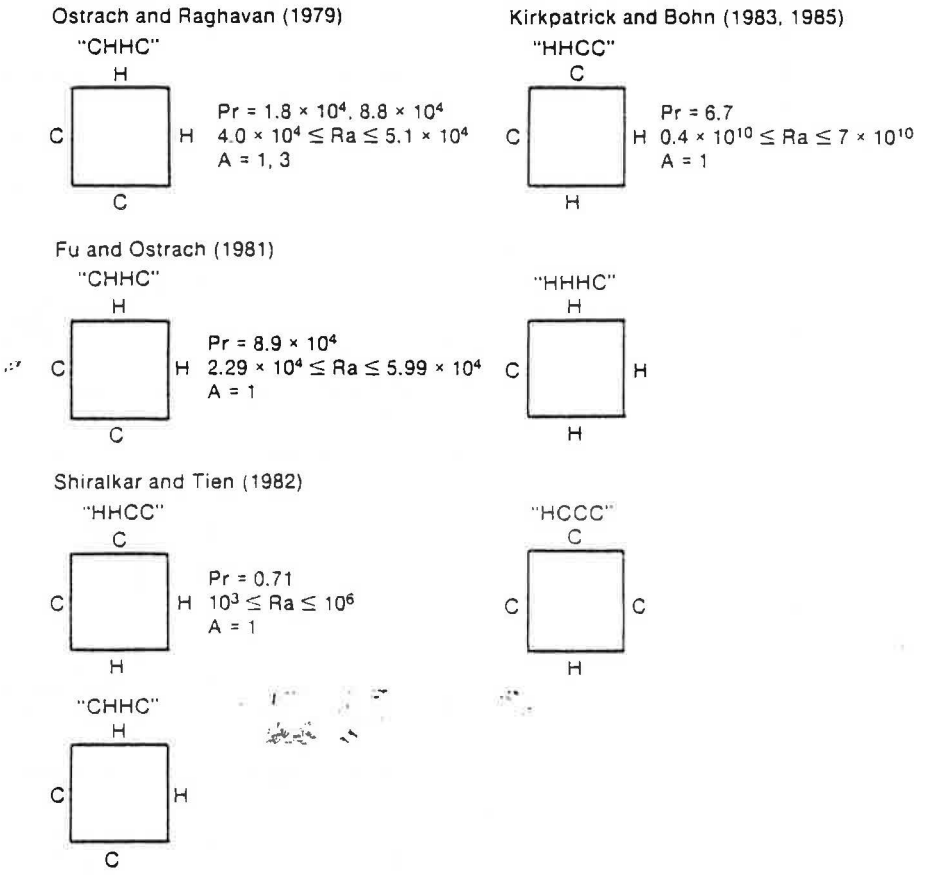

Figure 9. **Summary of enclosure correction studies with vertical and horizontal heat fluxes**

by Anderson and Lauriat is shown in Figure 10. They compared their heat transfer results to correlations for horizontal and vertical surfaces in unconfined flows. The unconfined flow correlations overpredicted heat transfer from the vertical wall by 13% and underpredicted heat transfer from the floor by 40%.

Anderson, Fisher, and Bohn experimentally examined the flow structure, heat transfer, thermal stratification, and temperature distributions in an enclosure with a heated floor and heated and cooled side walls. During their experiments they varied the relative level of heating to the floor and one vertical wall between the range $0 \leq$

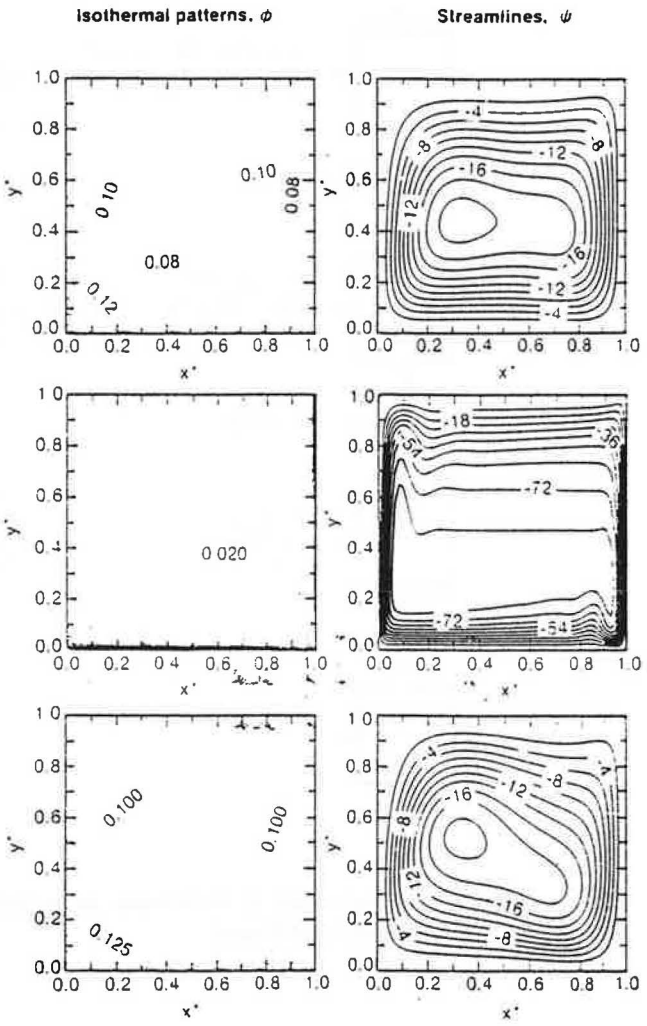

Figure 10. **Streamlines and isotherms showing the structure of the horizontal boundary layer flow next to the heated floor of an enclosure with an insulated ceiling**

PWR ≤ ∞. The parameter PWR is the ratio of the energy per unit area convected from the floor divided by the energy per unit area convected from the vertical wall. When PWR = 0, the problem becomes that of a closed cavity with differentially heated end walls. When PWR = ∞, the problem reduces to that of a cavity with a heated floor and a cooled vertical wall studied by Anderson and

Lauriat. Anderson, Fisher, and Bohn (1985b) found the level of the thermal stratification in the cavity to be a strong function of the level of heating provided to the floor (Figure 11). The minimum level of thermal stratification occurred for floor heating only (PWR = ∞). Anderson, Fisher, and Bohn (1985b) used these results to calculate the total convection energy transport from the hot walls to the cold wall over the range $0 \leq PWR \leq 4$. Their results are plotted in Figure 12. The convective transport for PWR = 4 was found to be a factor of two smaller than the convective transport for PWR = 0.

Anderson, Fisher, and Bohn concluded that floor heating decreases thermal stratification and decreases convective energy transport to the cold wall while side wall heating increases thermal stratification and increases convective energy transport to the cold wall. For applications where the cold wall represents a heat loss, floor heating is more effective than side wall heating because it minimizes energy losses. However, if the cold wall represents a convectively coupled thermal storage wall, then convective transport to the storage wall is maximized by absorbing incoming solar energy on a vertical surface rather than on the floor.

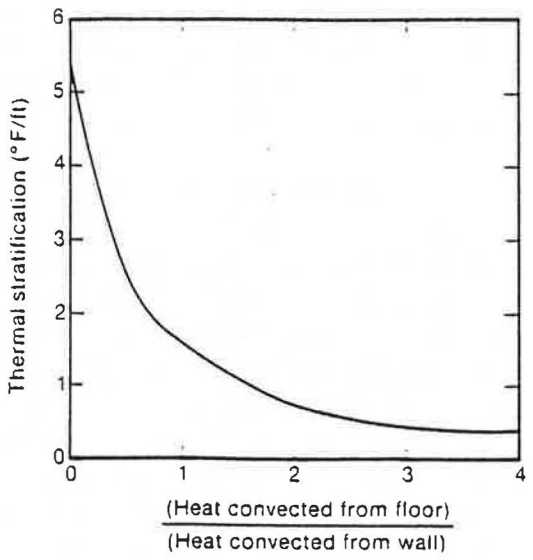

Figure 11. Effect of floor heating on thermal stratification in a single zone with a cold wall

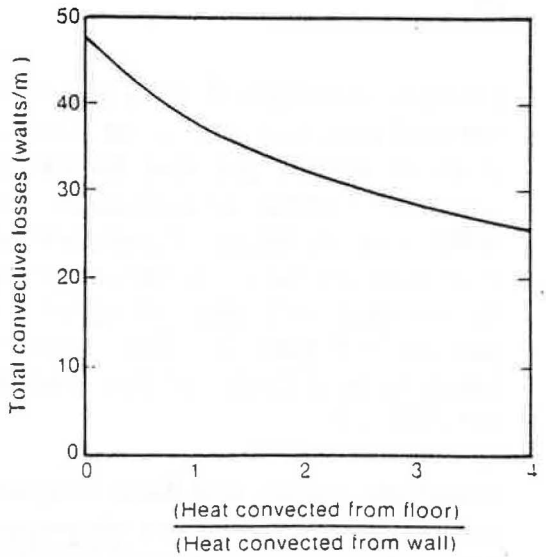

Figure 12. Effect of floor heating on convective coupling to a cold vertical surface

Effects of Surface Roughness

Room surfaces can have uniformly distributed roughness elements, as in the case of a masonry wall, or can have isolated projections due to window sills, door soffits, or ceiling beams. Anderson and Bohn (1984) examined the effect of distributed roughness elements on heat transfer from a vertical wall. They found the roughness elements were most effective on an isothermal wall, producing an average increase in total heat transfer of 10% to 15% and a local increase of as much as 40%.

The influence of the roughness elements on the onset of transition to turbulent flow is shown in Figures 13 and 14 for isothermal and constant flux thermal boundary conditions. The roughness caused the boundary layers to undergo transition slightly sooner than they would on a smooth surface. The boundaries of the cross-hatched area on Figure 14 are the locations of transition measured by Jaluria and Gebhardt (1974) on a vertical plate in an unconfined medium. The solid lines on Figures 13 and 14 indicate the location of transition in the absence of roughness. It can be seen from Figure 14 that transition in enclosures with heated and cooled vertical walls is delayed by about an order of magnitude as compared to transition on

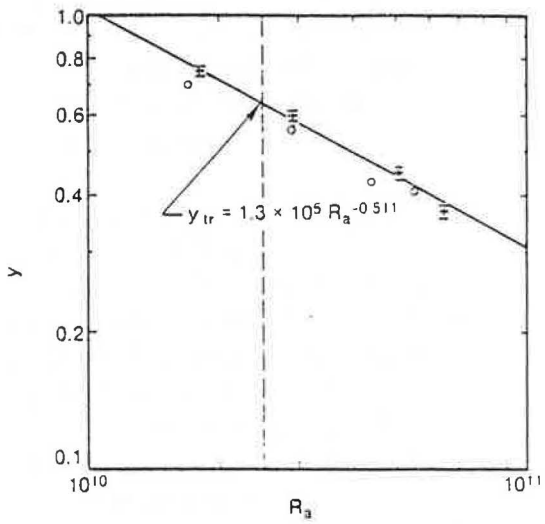

Figure 13. Effect of surface roughness on onset of transition from laminar to turbulent flow for an isothermal wall boundary condition
O = rough surface $\overline{+}$ = smooth surface (lines above and below are error bars; solid line indicates the location of transition in the absence of roughness)

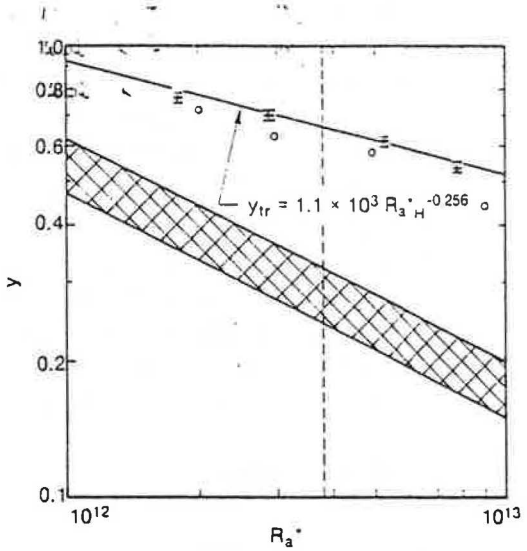

Figure 14. Effect of surface roughness on onset of transition from laminar to turbulent flow for a constant flux wall thermal boundary condition
0 = rough surface $\overline{+}$ = smooth surface (lines above and below are error bars; boundaries of cross-hatched area are the locations of transition measured by Jaluria and Gebhardt (1974) on a vertical plate in an unconfined medium; solid line indicates the location of transition in the absence of roughness)

an isolated vertical surface. The primary reason for this delay in transition is the large level of thermal stratification in the core of the enclosure flow. This thermal stratification stabilizes the boundary layer by reducing the buoyancy force when compared to an external flow in isothermal surroundings.

Finite size roughness elements in natural convection flows have been considered by Nansteel and Greif (1984); ElSherbiny, Hollands, and Raithby (1978); Al-Arabi and El-Rafaee (1978); and Shakerin, Bohn, and Loehrke (1986). Nansteel and Greif examined downward projections similar to door soffits and found regions of intense turbulence downstream of the projection at $Ra_L = 10^{11}$. These turbulent regions did not exist if the projection extended across the entire width of the enclosure. ElSherbiny, Hollands, and Raithby considered an enclosure with one V-corrugated and one flat surface. They found heat transfer to increase by up to 50% over that for an enclosure with two smooth surfaces. Al-Arabi and El-Rafaee studied natural convection from an isolated V-corrugated plate. They compared the heat transfer results of the V-corrugated plate to a finned plate and found that the corrugated plate provided higher heat transfer than a finned plate with a weight that equalled the weight of the V-corrugated plate. Shakerin, Bohn, and Loehrke experimentally and numerically studied the changes in heat transfer produced by horizontal rectangular fins attached to a vertical heated wall in an enclosure. They found that even a perfectly conducting fin did not produce a significant increase in convective heat transfer. When the spacing between the fins was reduced below the height of the fins, they found the flow was far less able to penetrate the space between the fins. The surface heat flux in the stagnant region between closely spaced fins was reduced so that even though the total surface area of the finned wall was larger than that of a smooth wall, the total heat convective transfer rate was nearly the same.

Triangular Enclosures

Most of the natural convection studies applicable to building heat transfer have been on rectangular enclosures. Triangular spaces can occur in A-frames, rooms with clerestories, and rooms with vaulted ceilings. Flack, Konopnicki, and Rooke (1979); Flack (1980); and Poulikakos and Bejan (1983a) have conducted experimental studies of triangular enclosures. In addition, Akinete and Coleman (1982) and

Poulikakos and Bejan (1983b) have conducted numerical studies of natural convection in triangular enclosures.[5]

NATURAL CONVECTION HEAT TRANSFER BETWEEN BUILDING ZONES

Heat transfer between rooms in passive solar buildings is caused almost entirely by natural convection when the area of the flow connection or doorway is much smaller than the overall cross-sectional area of the room. Two major mechanisms can be responsible for natural convection flow between building zones:

(1) bulk density differences created by air temperature differences between hot and cold zones and

(2) thermosiphon "pumping" produced by the boundary layers that form next to heated and cooled surfaces.

Natural convection flows in solar buildings generally result from a combination of boundary layer flows and bulk density differences.

Flows Driven by Bulk Density Differences

Studies that examine flow driven by bulk density differences include those of Emswiler (1926), Brown and Solvason (1962), and Graf (1964). Emswiler calculated the flow between zones for a partition with multiple openings by using Bernoulli's equation but did not treat the heat transfer aspects of the problem. Brown and Solvason measured heat transfer in an air-filled enclosure that was divided into hot and cold regions by a single partition with a variable size opening. Using inviscid calculations and assuming isothermal fluid reservoirs on either side of the partition, they predicted that heat transfer through the partition would be correlated by a relationship of the form

$$Nu = \frac{C}{3}\left(\frac{w}{W}\right)\left(\frac{h}{H}\right)^{3/2}\ (Ra\ Pr)^{1/2}\ . \qquad (13)$$

The constant C appearing in Equation 13 is the discharge coefficient for the aperture and has values $C \geq 0.6$ for high flow rates (Lienhard and Lienhard, 1984). Balcomb, Jones, and Yamaguchi (1984) recommend the value $C = 0.611$. Kirkpatrick, Hill, and Burns (1986) found

values of $0.65 \leq C \leq 0.75$, based on measurements taken in a full-scale building. The parameters h/H and w/W that appear in Equation 13 are the ratios of doorway height to total room height and doorway width to room width, respectively. The temperature difference used in the definition of Nu and Ra in Equation 13 is the temperature difference between the fluid in the hot and cold zones.

Graf used inviscid calculations to examine mixed forced and free convection flow by adding the pressure contribution from the forced flow to the pressure difference produced by the density differences between the fluid reservoirs. Figure 15 demonstrates the types of flow profiles that result from the inviscid calculations. Balcomb and Yamaguchi (1983) have demonstrated that skew velocity profiles similar to Figure 15 can also occur in multilevel passive solar buildings without the presence of a forced flow because of the complex flow paths created by hallways, stairways, and doors.

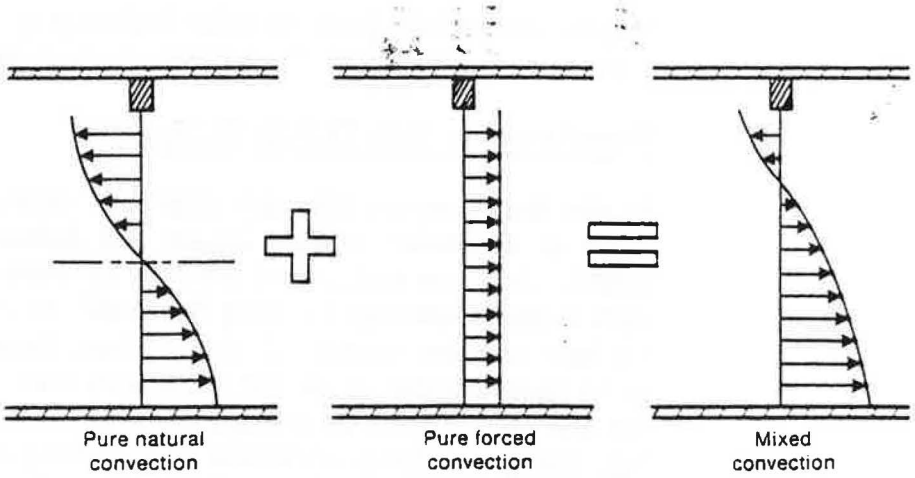

Figure 15. Interzone flow profiles predicted by using Bernoulli's equation and assuming isothermal fluid reservoirs on either side of the partition. The combination of a forcing pressure in addition to the density difference between the fluid reservoirs produces a skewed velocity profile.

Flows Driven by Boundary Layer Pumping

Many quantitative studies have been done of simple interzonal natural convection flows for the case when the flow between zones is driven entirely by boundary layers. Two-dimensional partitions have been considered by Janikowski, Ward, and Probert (1978); Bejan and Rossie (1981); Nansteel and Greif (1981 and 1984); Bajorek and Lloyd (1982); Chang, Lloyd, and Yang (1982); and Lin and Bejan (1983). All these studies were experimental except that of Chang, Lloyd, and Yang, which was a finite difference model of a geometry similar to the experimental work of Bajorek and Lloyd. Lin and Bejan provide a perturbation solution valid in the limit $Ra \to 0$ in addition to their experimental results. The only three-dimensional study is that of Nansteel and Greif, who consider a partition with a rectangular opening. Figure 16 summarizes these papers. An interesting result of these studies is that a partition tends to damp out the flow in subregions that are subjected to stable thermal boundary conditions. This effect reduces the effective wall area exposed to the primary flow, as can be seen in the flow patterns observed by Bejan and Rossi, Nansteel and Greif, and Lin and Bejan. This reduction in actively participating surface area produces a proportional reduction in heat transfer when compared to an enclosure without intervening partitions. The reduction also leads to the formation of a relatively hot, stagnant layer of air near the ceiling of a sunspace if the height of the sunspace is larger than the height of the sunspace doorway.

Nansteel and Greif recommend the following relation for boundary-layer-driven heat transfer through a simple partition separating two rooms:

$$Nu = 0.915\ (h/H)^{0.401}\ Ra^{0.207} \tag{14}$$

for

$$1/4 \leq h/H \leq 1 \tag{15}$$

and

$$w/W \geq 0.093\ . \tag{16}$$

The temperature difference used in the evaluation of Nu and Ra in Equation 14 is the temperature difference between the hot and cold end walls of the enclosure.

Janikowski, Ward, and Probert (1978)

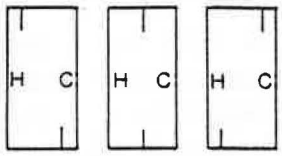

Air-filled, $Gr_L = 1.1 \times 10^6$
$H/L_{enclosure} = 5$

Bejan and Rossie (1981)

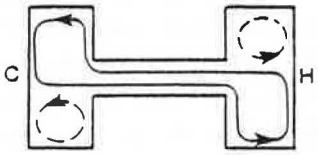

Water-filled, $5 \times 10^6 \leq Ra_H \leq 5 \times 10^7$
$H/L_{duct} = 1/6$

Nansteel and Greif (1981)

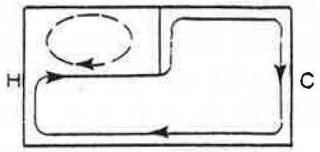

Water-filled, $2 \times 10^{10} \leq Ra_L \leq 1 \times 10^{11}$
$H/L_{enclosure} = 1/2$

Bajorek and Lloyd (1982)

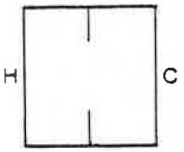

Air-filled, CO_2-filled, $10^5 \leq Gr_L \leq 3 \times 10^6$
$H/L_{enclosure} = 1$

Chang, Lloyd and Yang (1982)

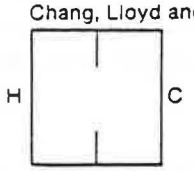

Air-filled, $10^3 \leq Gr_L \leq 10^8$
$H/L_{enclosure} = 1$

Lin and Bejan (1983)

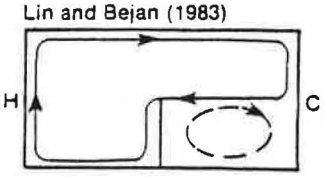

Water-filled, $10^9 \leq Ra_H \leq 10^{10}$
$H/L_{enclosure} = 0.31$

Nansteel and Greif (1984)

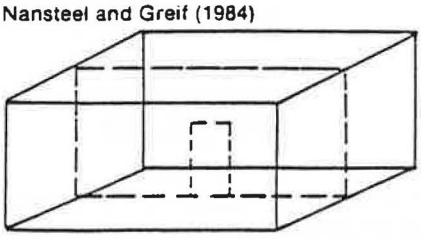

Water-filled, $10^{10} \leq Ra_L \leq 10^{11}$
$H/L_{enclosure} = 1/2$

Figure 16. Summary of interzone natural convection studies

Studies Conducted in Full-Scale Buildings

Studies of natural convection flows in full-scale buildings have been reported by Shaw (1971); Balcomb and Yamaguchi (1983); Balcomb, Jones, and Yamaguchi (1984); and Kirkpatrick, Hill, and Burns (1986). Shaw included the effects of forced air flow. Kirkpatrick, Hill, and Burns included these effects as well as examined the effect of thermal stratification on the flow between zones. Owing to the relatively low level of thermal stratification measured during their experiment, Kirkpatrick, Hill, and Burns found only a small difference between predictions based on stratified and isothermal models. Shaw and Kirkpatrick, Hill, and Burns conducted their measurements in an unoccupied building. Balcomb and Yamaguchi, and Balcomb, Jones, and Yamaguchi conducted measurements in a series of occupied houses encompassing a wide range of floor plans. Balcomb (1985) summarizes the results of these experiments.

These full-scale studies demonstrate that the bulk density model can be used to describe air flow between zones with large air temperature differences. Some disagreement exists concerning the correct temperature difference for Equation 13. Shaw used the temperature difference between the top and bottom of the doorway. Kirkpatrick, Hill, and Burns integrated the temperature difference measured at equal heights on either side of the doorway. Balcomb, Jones, and Yamaguchi used the temperature difference at midheight on either side of the doorway, with a correction factor to account for the difference between the room-to-room temperature difference and the temperature difference between the top and bottom of the doorway. Experiments conducted in scale-model test cells by Weber and Kearney (1980) and Yamaguchi (1984) have examined the effects of various definitions of zone-to-zone temperature difference on the heat transfer results.

Jones, Balcomb, and Otis (1985) have developed a model for air transport in a two-zone enclosure with heated and cooled end walls similar to Figure 3b. The model incorporates features found from observations made in more than 12 full-scale buildings. Jones, Balcomb, and Otis found that sunspace glazing in direct sun is typically about 5°C (10°F) warmer than the sunspace air. This temperature difference was found to produce a strong upward boundary-layer flow on the glazing, which entrains cool air from the sunspace

core. Jones, Balcomb, and Otis measured velocities of 0.46 to 0.61 m/s (1.5 to 2.0 ft/s) in the glazing boundary layer and estimated that the sunspace glazing accounted for more than half of the heat flow from the sunspace into the remainder of the building during periods of strong solar heating. Their model couples the boundary layers that form on the heated and cooled end walls with a bulk density model for the flow through the aperture separating the hot and cold zones. Initial use of the model has been limited to the study of the transient flow that results when the door separating the hot and cold zones is suddenly opened.

Blockage of Boundary-Layer Flows

A comparison of Equations 13 and 14 demonstrates that the natural convection flow regime that governs the flow through the aperture (bulk-density driven or boundary-layer driven) strongly affects the geometric dependence of the heat transfer coefficient. In the bulk-density-driven regime (Equation 13), the heat transfer coefficient depends strongly on both the aperture height ratio h/H and the aperture width ratio w/W. In the boundary-layer-driven regime (Equation 14), the heat transfer coefficient depends weakly on the aperture height ratio and appears to be independent of the aperture width ratio. Because of these differences, one must be able to predict when a multizone flow is in the bulk-density-driven or boundary-layer-driven regime.

Nansteel and Greif (1984) have demonstrated that heat transfer between two zones in the boundary layer regime is nearly independent of the width of the aperture between zones for $w/W \geq 0.093$ and $0.25 \leq h/H \leq 1.0$. However, as the width of the aperture is reduced, the boundary layer flow will eventually be blocked. Flow blockage will result in the formation of large temperature differences across the aperture and cause a transition from boundary-layer-driven to bulk-density-driven convection.

The onset of boundary-layer flow blockage can be estimated by comparing the total cross-sectional area required by the boundary-layer flow to the area of the aperture between zones. If the aperture is smaller than the area required by the boundary-layer flow, then it will have to accelerate to pass through the aperture. The additional driving force required to convect the flow through the

aperture can only be provided by the creation of bulk density differences between the hot and cold zones of the enclosure.[6]

Scott, Anderson, and Figliola (1985) conducted an experimental investigation to determine the onset of blockage of natural convection boundary-layer flow in a two-zone cavity with differentially heated end walls. They varied the width of the aperture between the zones while measuring the heat transfer and temperature distributions within the cavity. Figure 17 shows the temperature difference between the hot and cold zone measured by Scott, Anderson, and Figliola as a function of the size of the aperture between zones, for a constant level of convective energy transport between zones. The temperature difference required to transport an equivalent amount of energy using bulk density differences is also shown in Figure 17, as calculated from Equation 13.

Scott, Anderson, and Figliola found that the boundary-layer flow studied during their experiment required a smaller zone-to-zone temperature difference than a flow driven by bulk density differences provided that the area of the flow aperture was larger than 2% of the total cross-sectional area of the enclosure. This result

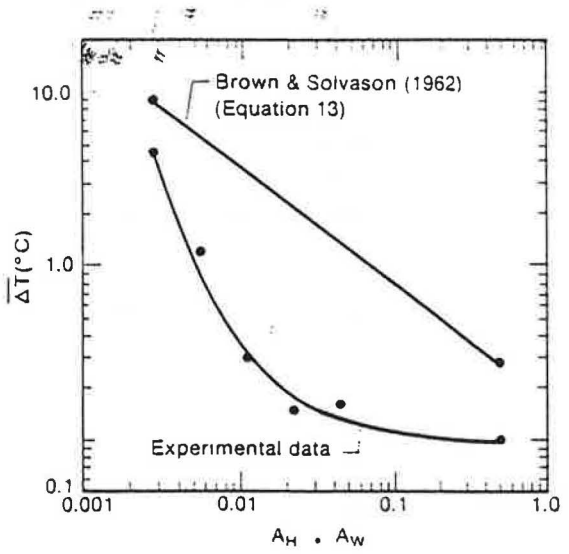

Figure 17. Temperature difference between hot and cold zones measured by Scott et al. (1985) shown as a function of aperture area.
$\overline{\Delta T}$ = fluid temperature difference between hot and cold zones.

suggests that substantial benefits can be associated with the use of boundary layer flows, particularly in retrofit applications where flow aperture areas are limited.

Trombe Walls and Thermosiphoning Air Panels

The two-zone studies described above assumed that the zones on either side of the dividing partition have aspect ratios of order one. In Trombe walls and thermosiphoning air panels, the width of the direct-gain zone is reduced until it becomes a vertical duct bounded by the window surface and the absorbing wall surface.[7]

Sparrow and Azevedo (1985) experimented with the effect of channel width on natural convection heat transfer between vertical parallel plates. They found that heat transfer was reduced dramatically if the width of the channel had the same order of magnitude as the boundary-layer thickness. The reduction in convection heat transfer measured during their experiment is plotted as a function of channel spacing in Figure 18. Sparrow and Azevedo were able to

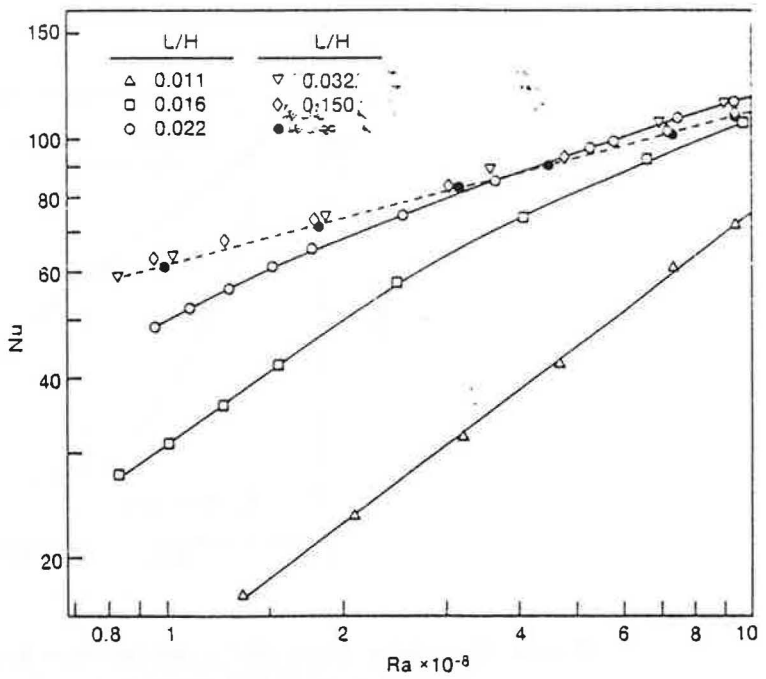

Figure 18. Effect of spacing on heat transfer in a parallel plate channel

reduce all their data to a single curve by plotting the data as shown in Figure 19. Their final correlation for heat transfer over the entire range of plate spacing $0.011 \leq L/H \leq 0.5$ is

$$Nu_L = \left\{ \left(\frac{12}{L/H\ Ra_L} \right)^2 + \left(\frac{1}{0.619\ (L/H\ Ra_L)^{1/4}} \right)^2 \right\}^{-1/2}. \quad (17)$$

To avoid blockage of the flow through the duct, Sparrow and Azevedo found that the channel width should satisfy the following inequality, for a channel that was heated along one wall:

$$L/H\ Ra^{1/4} \geq 5 . \quad (18)$$

For Trombe wall and thermosyphoning air panel applications where heating occurs on both walls, this guidance should be multiplied by a factor of two:

$$L/H\ Ra^{1/4} \geq 10 . \quad (19)$$

For a Trombe wall with $Ra = 10^{10}$ and $H = 2.4$ m (8 ft), Equation 19 gives a recommended Trombe wall channel spacing of

$$L \geq 3 \text{ in.} \quad (20)$$

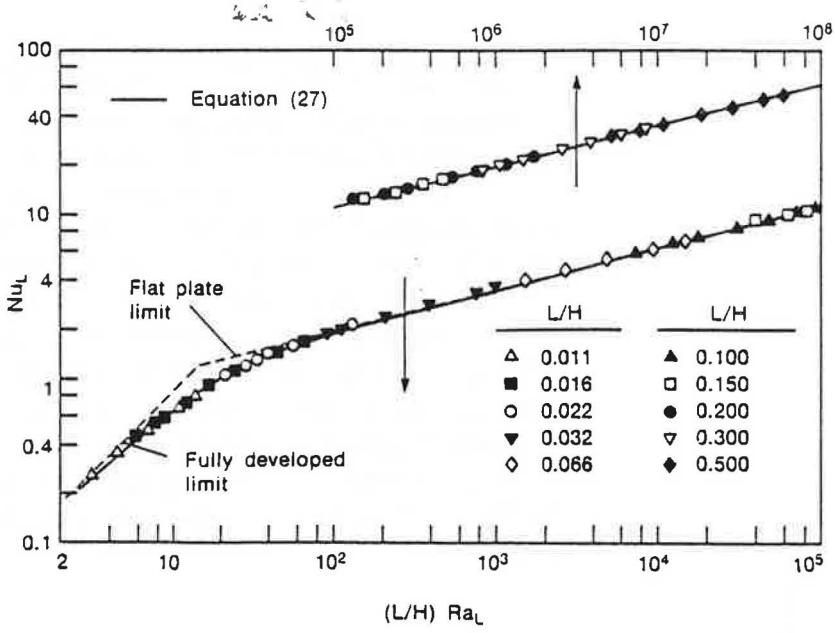

Figure 19. Heat transfer in a parallel plate channel

Sparrow and Azevedo did not examine the effect of entrance and exit losses during their study; therefore, Equations 18 and 19 should not be used to size entrance and exit apertures for Trombe wall and thermosiphoning air-panel applications.

Recommendations for Future Research

A preliminary understanding has been developed of the factors that govern natural convection transport in solar buildings. However, several applied and fundamental research areas still require further work:

a) Advanced building materials. The development of advanced building materials, such as fenestrations with switchable transmissivities and drywall incorporating phase-change thermal-storage materials, promises to give the thermal designer tremendous control over the distribution of solar gains and the placement of thermal storage in solar buildings. A critical need exists for the development of design guidelines to ensure that the performance of these advanced materials is not limited by heat transfer. Phase-change drywall will not perform well if convective coupling is inadequate. Many of the switchable fenestrations can be highly absorptive and may cause overheating in some applications.

b) Mixed forced/free convection in solar building components. Natural convection is an effective mechanism for energy transport in solar buildings. However, performance can be improved by using forced flows to aid natural convection. The performance of many hybrid solar building systems has been disappointing (Balcomb, 1985). Comprehensive design guidelines are needed for sizing of apertures, fans, and baffles in hybrid solar building components such as wall-attached air panels and hot-air redistribution systems. In addition, convective coupling to thermal storage in ventilation cooling applications is not well understood. A recent study by Johnson, Neiswanger, and Casey (1986) demonstrates that the level of convective coupling can vary by as much as a factor of three, depending on the location on the thermal storage wall.

c) Thermal stratification and overheating in atria and sunspaces. Overheating reduces thermal comfort and increases thermal losses in solar buildings. Well-designed sunspaces are generally only 25% efficient. Daylighting in large atria can result in excess solar gains that must be removed by increasing the capacity of the HVAC system. Additional study is required to improve the thermal performance of atria and sunspaces by increasing our understanding of the mechanisms that produce thermal stratification and overheating problems.

d) Boundary layer energy transport. Preliminary research results suggest that multizone flows driven by boundary layers will not be blocked as long as the flow aperture area is not reduced below 2% of the solar aperture area. Design guidelines based on bulk-density driven flow suggest that the flow aperture area should not be reduced below 15% of the solar aperture area. The smaller aperture areas required by boundary layer flows can provide additional architectural freedom, particularly in retrofit applications where flow aperture area may be limited. Additional research is necessary to provide design guidelines for the use of boundary layer transport in multizone building flows.

A substantial level of research effort is currently being conducted in the areas described above by solar researchers as well as by researchers in the related fields of smoke and fire spread, indoor air quality, and cooling of electronic equipment. The widespread use of microcomputers should make it fairly easy to adapt the thermal design algorithms developed by these researchers into a form that can be easily used by architects, builders, and designers.

NOTES

[1] The radiation heat loss has been calculated by assuming that the window and room can be modeled as ideal black surfaces. The radiative heat transfer coefficient $\bar{h}_{rad}$ used in Figure 5 is defined as:

$$\bar{h}_{rad} = \sigma \frac{(T_H^4 - \bar{T}_{Window}^4)}{(T_H - T_C)} \qquad (21)$$

where σ is the Stefan-Boltzman constant and $\bar{T}_{window}$ is the average temperature of the window surface. T_H is the internal (hot) temperature, and T_C is the external (cold) temperature. For the case of zero external wind the average window temperature is

$$\bar{T}_{window} = \frac{(T_H + T_C)}{2} . \tag{22}$$

For the case of high external wind it was assumed that

$$\bar{T}_{window} = T_C . \tag{23}$$

The internal temperature T_H is assumed to be constant at 20°C (68°F). The natural convection heat transfer coefficient used in Figure 5 for the case of zero external wind is based on the conjugate conductive/convective analysis of Anderson and Bejan (1980 and 1981). The natural convection heat transfer coefficient used in Figure 5 for the case of high external wind is based on the boundary layer analysis of Gill (1966) and Bejan (1979) under the assumption that the window surface temperature approaches the external air temperatures.

[2]The constant height H/variable spacing L case considered by Korpela, Lee, and Drummond (1982) is distinct from the constant L/variable H case previously considered by Bejan (1980). Bejan's analysis assumes boundary layer flow and considers the dependence of Nu_L on aspect ratio with fixed plate spacing L and variable height H. Korpela, Lee, and Drummond limit their study to the consideration of Ra numbers in the transitional region between conduction- and boundary-layer-dominated heat transfer and consider the dependence of Nu on aspect ratio with fixed H and variable L. Their results can be used to determine the Ra,A combination, which produces minimum heat transfer at fixed H, while Bejan's analysis allows one to determine the Ra_L,A combination producing maximum heat transfer at fixed L.

[3]If this scaling is not observed, the heat transfer from a vertical surface in an enclosure with complicated boundary conditions on its vertical walls can appear to be drastically different from that in an enclosure where one vertical surface is uniformly heated and one vertical surface is uniformly cooled. For example, in a cubical enclosure with four vertical walls, three hot (T_H) and one cold (T_C), the bulk temperature difference for the cold wall is

$$\Delta T_b = \frac{\Delta T}{4} \tag{24}$$

where

$$\Delta T = T_H - T_C . \tag{25}$$

The overall heat transfer to the cold wall has to be the same regardless of the temperature difference used in the definition of the heat transfer coefficient. This implies that

$$\bar{h}_b \, \Delta T_b = \bar{h} \, \Delta T \tag{26}$$

or

$$\frac{\bar{h}}{\bar{h}_b} = \frac{\Delta T_b}{\Delta T} = \frac{1}{4} . \tag{27}$$

Equation 27 indicates that the heat transfer coefficient based on ΔT will be four times smaller than the heat transfer coefficient based on ΔT_b for the three-heated and one-cooled wall geometry described above. This apparent discrepancy is a result of the choice of the temperature difference used in the definition of the heat transfer coefficient and does not indicate a drastic change in the convective heat transfer mechanism. If ΔT_b is used rather than ΔT, the heat transfer coefficient does not change significantly regardless of the thermal boundary conditions on the vertical walls of the enclosure.

[4]Ostrach and Raghavan (1979) studied the configuration CHHC for high Prandtl silicone oils in enclosures with aspect ratios of one and three. Here H refers to a heated wall and C refers to a cooled wall. The notation scheme begins with the floor, the righthand vertical side wall, the top, and then the lefthand vertical side wall. The two remaining vertical side walls were insulated. Ostrach and Raghavan found that heating of the top wall and cooling of the bottom wall reduced the vertical velocity near the vertical wall. Fu and Ostrach (1981) examined the same heating configuration as Ostrach and Raghavan but considered the effect of symmetric as well as asymmetric heating. Symmetric heating occurs when $(T_T + T_B)/2 = (T_H + T_C)/2$. They found that the symmetrical case produced the greatest reduction in the vertical velocity. Shiralkar and Tien (1982) conducted numerical studies of stable and unstable heating corresponding to configurations CHHC and HHCC. Shiralkar and Tien did not observe any thermal instabilities such as Benard cells or thermal plumes when the enclosure was subjected to unstable heating (configuration CHHC), but the temperature distribution in the core was found to be strongly dependent on the heating configuration. Stable heating (configuration HHCC) produced a motionless core with a high level of thermal stratification. Unstable heating induced motion in the core, making it almost isothermal. Kirkpatrick and Bohn (1983 and 1986) conducted a series of experiments in a water-filled cubical enclosure that was heated from below while the thermal boundary conditions on two side walls and the top wall of the enclosure were varied. Kirkpatrick and Bohn tested three configurations: HHCC, HHHC, and HCCC. They conducted their study at Rayleigh numbers four orders of magnitude higher than any previous studies. They found the thermal boundary condition on the top wall of the enclosures to strongly influence the temperature distribution and flow structure in the enclosure. When both the floor and the ceiling were heated, they found the fluid in the core was highly stratified. When the floor was heated and the ceiling was cooled, turbulent thermal plumes were generated at the top and bottom surfaces of the enclosure and the thermal stratification of the core was destroyed.

[5]Flack, Konopnicki, and Rooke measured the heat transfer in an air-filled isosceles triangular enclosure by using an interferometer. The base of the enclosure was insulated and the enclosure had one isothermal-heated and one isothermal-cooled upper wall. Flack, Konopnicki, and Rooke found the average Nusselt number to be within 10% to 20% of the values for a rectangular enclosure but found a strong conduction-dominated region near the apex of the enclosure because of the physical proximity of the hot and cold surfaces in that region. This conduction-dominated region caused a sharp increase in heat transfer on the hot wall near the apex.

Flack used the same apparatus previously used by Flack, Konopnicki, and Rooke to examine the case when both of the upper sides of the enclosure were the same temperature while the floor of the enclosure was maintained at a different temperature. For stable heating (hot ceiling-cold floor), the heat transfer varied at most by 10% from a pure conduction solution. Four horizontally aligned Benard cells formed along the long axis of the enclosure during unstable heating (hot base-coid sides). The axis of rotation of the Benard cells was perpendicular to the long axis of the enclosure. Poulikakos and Bejan considered natural convection in an air-and-water filled, unstably heated, right triangular enclosure. The flow was found to be turbulent during the water experiments owing to the higher Rayleigh numbers that were achieved in their apparatus.

Akinete and Coleman conducted a numerical study on a stably heated, right triangular enclosure for the range $800 \leq Gr_L \leq 6400$, $0.0635 \leq A \leq 1$ and $Pr = 0.733$. They found a drastic drop in heat transfer as the aspect ratio was increased, indicating that the heat transfer process was conduction dominated. The same conduction-dominated behavior was observed by Flack in stably heated, isosceles triangular enclosures. Poulikakos and Bejan conducted a two-dimensional transient numerical study of an isosceles triangular enclosure with cold upper sides and a warm base. Their calculation assumed that the fluid in the enclosure was initially isothermal at the base temperature T_H. At time $t = 0$ the upper sides of the enclosure were suddenly cooled to T_C. For high-aspect ratio enclosures the transient Nusselt numbers initially overshot their steady-state values. The numerical solution of Poulikakos and Bejan assumed two symmetrical axially oriented rolls in contrast to the transversely oriented rolls observed by Flack.

[6]The flow area A_{bl} required by the boundary layers on heated and cooled surfaces can be calculated by summing the product of the thickness and width of each boundary layer in the enclosure:

$$A_{bl} = \sum_{n=1}^{N} (\delta W)_n \, . \tag{28}$$

According to the model described above, flow blockage will occur when

$$\frac{A_{bl}}{\ell w} = \frac{\sum_{n=1}^{N} (\ell W)_n}{\ell w} \geq 1 \, . \tag{29}$$

For laminar flow the natural convection boundary-layer thickness next to a vertical surface is scaled by the relationship (Bejan, 1984)

$$\frac{\delta}{H} \sim \frac{1}{Ra_H^{*1/5}} . \tag{30}$$

If we assume that the height, width, and average heat flux from each active surface are the same, with the values H, W, and q", respectively, then the flow blockage criteria expressed by Equation 29 can be rearranged into the simple form

$$\frac{h}{H} \cdot \frac{w}{W} \sim \frac{N}{Ra_H^{*1/5}} . \tag{31}$$

The quantity Ra_H^*, which appears in Equations 30 and 31, is the flux modified Rayleigh number and is defined by Equation 2. The lefthand side of Equation 31 is the ratio of the area of the aperture to the cross-sectional area of the room, and N is the number of active heat transfer surfaces in the room. Equation 31 predicts that the onset of flow blockage is directly proportional to the number of active heat transfer surfaces and is inversely proportional to the Rayleigh number, which characterizes the natural convection flow. In simple terms, Equation 31 predicts that a small volume of hot air is less subject to flow blockage than a large volume of warm air.

[7] Elenbaas (1942) and Ostrach (1952) performed the first studies of natural convection in the duct formed by two vertical parallel surfaces. Studies with specific applications to solar buildings have been done by Akbari and Borgers (1979); Allen and Hayes (1985); Tasdemiroglu, Berjano, and Tinaut (1985); and Ormiston, Raithby, and Hollands (1985). Bodoia and Osterle (1962) considered the problem of developing flow between two isothermal plates with the same temperature. Miyatake and Fujii (1972) and Miyatake, Fujii, Fujii, and Tanaka (1973) calculated developing flow between two vertical plates when one plate was insulated and the other was an isothermal or constant flux surface. Aung, Fletcher, and Sernas (1972) conducted a numerical and experimental investigation of developing natural convection flow in a vertical duct with asymmetric side-wall heating for both constant heat flux and constant temperature boundary conditions. Kettleborough (1972) used an elliptic calculation method and found that regions of reverse flow could exist, particularly at high Rayleigh numbers. Sparrow, Chrysler, and Azevedo (1984) observed flow reversals near the exit of a vertical channel with one insulated side wall and one isothermal side wall, but found that the average Nusselt number was unaffected by the presence of the recirculating zone. Sparrow, Shah, and Prakash (1980) considered natural convection combined with radiation in a vertical channel with one insulated wall and one isothermal wall. They found that the radiative transport between the walls increased the convective heat transfer by 50% to 70% for $1.1 \le T_W/T_\infty \le 1.25$.

NOMENCLATURE

A = aspect ratio, H/L

B = constant vertical temperature gradient in tall vertical slot

Bi = wall Biot Number, $\frac{k_w t}{k_f H}$

c_p = specific heat at constant pressure

h = doorway height

$\bar{h}$ = convective heat transfer coefficient, $\frac{q}{HL\Delta T}$

H = enclosure height

L = spacing between enclosure walls

Pr = Prandtl Number, $\frac{\mu c_p}{k}$

q = total heat transfer across cavity

T = temperature

ΔT = $T_H - T_C$

α = thermal diffusivity, $\frac{k}{\rho c_p}$

ν = kinematic viscosity, $\frac{\mu}{\rho}$

μ = viscosity

Subscripts

b = bulk value

B = bottom wall

BL = boundary layer

C = cold vertical wall or cold fluid reservoir

DR = doorway

H = hot vertical wall or hot fluid reservoir

L = based upon the length scale L

rad = radiation

tr = location of transition

T = top

u = horizontal component of velocity

v = vertical component of velocity

x = horizontal distance or coordinate

y = vertical distance or coordinate

Ra = Rayleigh Number, $\frac{g\beta H^3 \Delta T}{\nu\alpha}$

Ra* = modified Rayleigh Number, $\frac{g\beta H^4 q''}{\nu\alpha R}$

Nu = Nusselt Number, $\frac{hH}{k}$

Greek

β = coefficient of thermal expansion

σ = Stephan-Boltzman constant

δ = boundary layer thickness

REFERENCES

Akbari, H., and T.R. Borgers, 1979. Free convective laminar flow within the Trombe wall channel. Solar Energy 22:165-174.

Akinete, V.A., and T.A. Coleman, 1982. Heat transfer by steady laminar free convection in triangular enclosures. Int. J. Heat Mass Transfer 25: 991-998.

Al-Arabi, M., and M.M. El-Rafaee, 1978. Heat transfer by natural convection from corrugated plates to air. Int. J. Heat Mass Transfer 21:357-359.

Allen, T., and J. Hayes, 1985. Measured performance of thermosiphon air panels. In Proc. of the 10th National Passive Conf. Boulder, CO: ASES. pp. 442-447.

Altmayer, E.F., A.J. Gadgil, F.S. Bauman, and R.L. Kammerud, 1983. Correlations for convective heat transfer from room surfaces. ASHRAE Transactions 89:Part 2A, 61-77.

Anderson, R., and A. Bejan, 1980. Natural convection on both sides of a vertical wall separating fluids at different temperatures. J. Heat Transfer 102:630-635.

Anderson, R., and A. Bejan, 1981. Heat transfer through single and double vertical walls in natural convection: theory and experiment. Int. J. Heat Mass Transfer 24:1611-1620.

Anderson, R., and M. Bohn, 1984. Heat transfer enhancement in natural convection enclosure flow. ASME Winter Annual Meeting, New Orleans.

Anderson, R., E.M. Fisher, and M. Bohn, 1985a. Natural Convection in a Closed Cavity with Variable Heating of the Floor and One Vertical Wall. SERI/PR-252-2591, Golden, CO: SERI.

Anderson, R., E. Fisher, and M. Bohn, 1985b. Thermal Stratification in Direct Gain Passive Heating Systems with Variable Heating of the Floor and One Vertical Wall. SERI/TP-252-2767, Golden, CO: SERI.

Anderson, R., and G. Lauriat, 1986. The horizontal natural convection boundary layer regime in a closed cavity. In Proc. of 8th Int. Heat Transfer Conf., San Francisco, CA.

Aung, W., L.S. Fletcher, and V. Sernas, 1972. Developing laminar free convection between vertical flat plate with asymmetric heating. Int. J. Heat Mass Transfer 15:2293-2308.

Bajorek, S.M., and J.R. Lloyd, 1982. Experimental investigation of natural convection in partitioned enclosures. J. Heat Transfer 104:527-532.

Balcomb, J.D., 1981. Passive solar energy systems for buildings. Solar Energy Handbook, Jan F. Kreider and Frank Kreith, eds. New York: McGraw-Hill, pp. 16-27.

Balcomb, J.D., 1985. Heat Distribution by Natural Convection: Interim Report. Los Alamos, NM: Los Alamos National Laboratory.

Balcomb, J.D., G.F. Jones, and K. Yamaguchi, 1984. Natural convection airflow measurement and theory. In Proc. of Ninth National Passive Solar Conf., Columbus, OH. Boulder, CO: ASES.

Balcomb, J.D., and K. Yamaguchi, 1983. Heat distribution by natural convection. In Proc. of the 8th National Passive Solar Conf., Santa Fe, NM. Boulder, CO: ASES.

Balvanz, J.L., and T.H. Kuehn, 1980. Effect of wall conduction and radiation on natural convection in a vertical slot with uniform heat generators on the heated wall. Natural Convection in Enclosures, ASME HTD 8:55-62.

Barakat, S.A., 1985. Inter-zone convective heat transfer in buildings: a review. In Heat Transfer in Buildings and Structures. P.J. Bishop, ed., ASME HTD 41:45-52.

Bauman, F., A. Gadgil, R. Kammerud, E. Altmayer, and M. Nansteel, 1983. Convective heat transfer in buildings: recent research results. ASHRAE Transactions 89:Part 1A, 215-230.

Bejan, A., 1979. Note on Gill's solution for free convection in a vertical enclosure. J. Fluid Mech. 90:561.

Bejan, A., 1980. A synthesis of analytical results for natural convection heat transfer across rectangular enclosures. Int. J. Heat Mass Transfer 23(5):723-726.

Bejan, A., 1984. Convection Heat Transfer. New York: John Wiley & Sons. p. 116.

Bejan, A., and A.N. Rossie, 1981. Natural convection in horizontal duct connecting two fluid reservoirs. J. Heat Transfer 103:108-113.

Bejan, A., and C.L. Tien, 1978. Laminar natural convection heat transfer in a horizontal cavity with different end temperatures. J. Heat Transfer 100C, 641.

Bodoia, J.R., and J.F. Osterle, 1962. The development of free convection between heated vertical plates. J. Heat Transfer 85:40-44.

Bohn, M.S., and R. Anderson, 1984. Influence of Prandtl Number on Natural Convection Heat Transfer Correlations. SERI/TR-252-2067, Golden, CO: SERI.

Bohn, M.S., and R. Anderson, 1986. Temperature and heat flux distributing in a natural convection enclosure flow. (to appear in J. Heat Transfer).

Bohn, M.S., A.T. Kirkpatrick, and D.A. Olsen, 1984. Experimental study of three-dimensional natural convection at high Rayleigh number. J. Heat Transfer 106:339-345.

Brown, W.G., and K.R. Solvason, 1962. Natural convection through rectangular openings in partitions--1. Int. J. Heat Mass Transfer 5:859-868.

Buchberg, H., I. Catton, and D.K. Edwards, 1976. Natural convection in enclosed spaces - a review of application to solar energy collection. J. Heat Transfer 98:182-188.

Catton, I., 1978. Natural convection in enclosures. 6th International Heat Transfer Conf., National Research Council of Canada.

Chang, L.C., J.R. Lloyd, and K.T. Yang, 1982. A finite difference study of natural convection in complex enclosures. 7th Int. Heat Transfer Conf.

Chao, P.K.-B., H. Ozoe, and S.W. Churchill, 1981. The effect of a nonuniform surface temperature on laminar natural convection in a rectangular enclosure. Chem. Eng. Commun. 9:245-254.

Chapman, A.J., 1974. Heat Transfer, 3rd edition, New York: MacMillan.

Cormack, D.E., L.G. Leal, and J. Imberger, 1974. Natural convection in a shallow cavity with differentially heated end walls--Part 1. Asymptotic theory, J. Fluid Mech. 65:209.

Elder, J.W., 1965. Laminar free convection in a vertical slot. J. Fluid Mech. 23:77.

Elenbaas, W., 1942. Heat dissipation of parallel plates by free convection. Physica 9:1.

ElSherbiny, S.M., K.G.T. Hollands, and G.D. Raithby, 1978. Free convection across inclined air layers with one surface V-corrugated. J. Heat Transfer 100:410-415.

ElSherbiny, S.M., G.D. Raithby, and K.G.T. Hollands, 1982. Heat transfer by natural convection across vertical and inclined air layers. J. Heat Transfer 104:96-102.

Emswiler, J.E., 1926. The neutral zone in ventilation. Trans. Amer. Soc. Heat Vent. Eng. 32:59-74.

Flack, R.D., 1980. The experimental measurement of natural convection heat transfer in triangular enclosures heated or cooled from below. J. Heat Transfer 102:770-772.

Flack, R.D., T.T. Konopnicki, and J.H. Rooke, 1979. The measurement of natural convective heat transfer in triangular enclosures. J. Heat Transfer 101:648-654.

Fu, B-I, and S. Ostrach, 1981. The effects of stabilizing thermal gradients on natural convection flows in a square enclosure. ASME HTD 16.

Gill, A.E., 1966. The boundary-layer regime for convection in a rectangular cavity. J. Fluid Mech. 26:515-536.

Graf, A., 1964. Theoretische Betrachtung uber den Luftaustauch zwischen zwei Raumen. Schweiz. Bl. Heiz. Luft 31:22-25.

Han, J.T., 1967. M.A. Science Thesis. Department of Mechanical Engineering, University of Toronto.

Jaluria, Y., and B. Gebhardt, 1974. On transition mechanisms in vertical natural convection flow. J. Fluid Mech. 66:309-339.

Jaluria, Y., 1982. Buoyancy-induced flow due to isolated thermal sources on a vertical surface. J. Heat Transfer 104:223-227.

Janikowski, H.E., J. Ward, and S.D. Probert, 1978. Free convection in vertical, air-filled rectangular cavities fitted with baffles. 6th Int. Heat Transfer Conf., Toronto.

Johnson, G.A., L. Neiswanger, V.P. Casey, 1986. Cross-flow mixed convection at high Rayleigh number in an open-ended rectangular enclosure. To be presented at 1986 ASME Winter Annual Meeting, Anaheim, CA, December 7-12.

Jones, G.F., J.D. Balcomb, and D.R. Otis, 1985. A model for thermally driven heat and air transport in passive solar buildings. ASME 85-WA/HT-69.

Kettleborough, C.F., 1972. Transient laminar free convection between heated vertical plates including entrance effects. Int. J. Heat Mass Transfer 15:883-896.

Kirkpatrick, A.T., and M.S. Bohn, 1983. High Rayleigh number natural convection in an enclosure heated from below and from the sides. ASME-AiChE National Heat Transfer Conf., Seattle, WA.

Kirkpatrick, A.T., and M.S. Bohn, 1986. An experimental investigation of mixed cavity natural convection in the high Rayleigh number regime. Int. J. Heat Mass Transfer 29(1):69-82.

Kirkpatrick, A., D. Hill, and P. Burns, 1986. Analysis and measurement of interzonal convection (to appear in J. Solar Energy Eng.).

Korpela, S.A., Y. Lee, and J.E. Drummond, 1982. Heat transfer through a double pane window. J. Heat Transfer 104:539-544.

Kubleck, K., G.P. Marker, and J. Straub, 1980. Advanced numerical computation of two-dimensional time-dependent free convection in cavities. Int. J. Heat Mass Transfer 23:203-217.

Lienhard V, J.H., and J.H. Lienhard IV, 1984. Velocity coefficients for free jets from sharp-edged orifices. J. Fluids Eng. 106:13-17.

Lin, N.N., and A. Bejan, 1983. Natural convection in a partially divided enclosure. Int. J. Heat Mass Transfer 26:1867-1878.

Lock, G.S.H., and R.S. Ko, 1973. Coupling through a wall between two free convective systems. Int. J. Heat Mass Transfer 16:2087-2096.

MacGregor, R.K., and A.F. Emery, 1969. Free convection through vertical plane layers--moderate and high Prandtl number fluids. J. Heat Transfer 91:391-403.

Miyatake, O., and T. Fujii, 1972. Free convection heat transfer between vertical parallel plates--one plate isothermally heated and the other thermally insulated. Heat Transfer Japanese Research 1:30-38.

Miyatake, O., T. Fujii, M. Fujii, and H. Tanaka, 1973. Natural convection heat transfer between vertical parallel plates--one plate with a uniform heat flux and the other thermally insulated. Heat Transfer Japanese Research 2:25-33.

Nansteel, M.W., and R. Greif, 1981. Natural convection in undivided and partially divided rectangular enclosures. J. Heat Transfer 103:623-629.

Nansteel, M.W., and R. Greif, 1984. An investigation of natural convection in enclosures with two- and three-dimensional partitions. Int. J. Heat Mass Transfer 27:561-571.

Newell, M.E. and F.W. Schmidt, 1970. J. Heat Transfer 92:159.

Ormiston, S.J., G.D. Raithby, and K.G.T. Hollands, 1985. Numerical Predictions of Natural Convection in a Trombe Wall System. ASME paper #85-HT-36.

Ostrach, S.. 1952. Laminar Natural Convection Flow and Heat Transfer of Fluids with and without Heat Sources in Channels with Constant Wall Temperature. NACA TN2863.

Ostrach, S., 1982. Natural convection heat transfer in cavities and cells. 7th Int. Heat Transfer Conf., Munich.

Ostrach, S., and C. Raghavan, 1979. Effect of stabilizing thermal gradients on natural convection in rectangular enclosures. J. Heat Transfer 101:238-243.

Ozoe, H., A. Mouri, M. Hiramitsu, S.W. Churchill, and N. Lior, 1984. Numerical calculation of three-dimensional turbulent natural convection in a cubical enclosure using a two equation model. In Fundamentals of Natural Convection/Electronic Equipment Cooling, L.C. Wilte and L.S. Saxena, eds., ASME HTD 32:25-32.

Poulikakos, D., and A. Bejan, 1983a. Fluid dynamics of an attic space. J. Fluid Mech. 131:251-269.

Poulikakos, D., and A. Bejan, 1983b. Natural convection experiments in a triangular enclosure. J. Heat Transfer 105:652-655.

Schinkel, W.M.M., and C.J. Hoogendoorn, 1983. Natural convection in collector cavities with an isoflux absorber plate. J. of Solar Energy Eng. 105:19-22.

Scott, D., R. Anderson, and R. Figliola, 1985. Blockage of Natural Convection Boundary Layer Flow in a Multizone Enclosure. SERI/TP-252-2847, Golden, CO: SERI.

Shaw, B.H., 1971. Heat and mass transfer by natural convection and combined natural convection and forced air flow through large rectangular openings in a vertical partition. Int. Mech. Eng. Conf. on Heat and Mass Transfer by Combined Forced and Natural Convection. Manchester, England.

Shiralkar, G.S., and C.L. Tien, 1982. A numerical study of the effect of a vertical temperature difference imposed on a horizontal enclosure. Numerical Heat Transfer 5:185-197.

Shakerin, S., M.S. Bohn, and R.L. Loehrke, 1986. Natural convection in an enclosure with discrete roughness elements on a vertical heated wall. 8th Int. Heat Transfer Conf., San Francisco, CA.

Sparrow, E.M., and L.F.A. Azevedo, 1985. Vertical channel natural convection spanning between the fully developed limit and the single-plate boundary-layer limit. Int. J. Heat Mass Transfer 28:1847-1857.

Sparrow, E.M., G.M. Chrysler, and L.F.A. Azevedo, 1984. Observed flow reversals and measured-predicted Nusselt numbers for natural convection in a one-sided heated vertical channel. J. Heat Transfer 106:325-332.

Sparrow, E.M., and C. Prakash, 1981. Interaction between internal natural convection in an enclosure and an external natural convection boundary-layer flow. Int. J. Heat Mass Transfer 24:895-907.

Sparrow, E.M., S. Shah, and C. Prakash, 1980. Natural convection in a vertical channel: I. Interacting convection and radiation. II. The vertical plate with and without shrouding. Numerical Heat Transfer 3:297-314.

Tasdemiroglu, E., F. Ramos Berjano, and D. Tinaut, 1985. The performance results of Trombe-wall passive systems under Aegean Sea climatic conditions. Solar Energy 30:181-189.

Viskanta, R., and D.W. Lankford, 1981. Coupling of heat transfer between two natural convection systems separated by a vertical wall. Int. J. Heat Mass Transfer 24:1171-1177.

Weber, D.D., and R.J. Kearney, 1980. Natural convective heat transfer through an aperture in passive solar heated buildings. In Proc. of 5th National Passive Conf., ASES: Boulder, CO, pp. 1037-1041.